SLAC-PUB-1227
(A)
April 1973

THE BEAM POSITIONS OF THE SPEAR STORAGE RING*

C. R. Carman and J.-L. Pellegrin

Stanford Linear Accelerator Center
Stanford University, Stanford, California 94305

ABSTRACT

The Stanford 2 GeV electron-positron storage ring is equipped with 20 beam position monitors. The principle of beam coupling is analysed and a calculation is made for the sensitivity to beam current and position, as well as for the intrinsic distortion of this type of monitor. Beam orbit coordinates are reconstructed by scanning the monitor's four electrode signals and the 20 stations around the machine. Normalization of the data and electronics nonlinearity compensation are one of the routine tasks of the computer control system.

(Submitted to Nucl. Instr. and Methods.)

* Work supported in part by the U. S. Atomic Energy Commission.

Introduction

The beam position monitoring system of the Stanford 2 GeV positron-electron storage ring comprises 20 identical monitor stations, approximately one every 12 meters, around the machine. The monitors are made of four small electrodes at 45^{o} over the horizontal, in order to clear the synchrotron radiation field. Coaxial relays at each station are used to multiplex the set of electrodes onto a trunk of four cables which run along each quadrant of the ring to the control room. Each beam position data is thus available under the form of four narrow pulses, typically 1 nsec wide, with a period of 790 nsec, that is, the period of revolution of the machine. The polarity of the pulses is the same as that of the beam. The beam coordinates at each station are obtained by measuring the relative amplitude of these four pulses. To this effect, the same electronics is used sequentially to produce a low frequency signal proportional to each electrode peak voltage. The data is then recorded, corrected and processed by a Sigma 5 computer which prints out the beam closed orbit coordinates. The complete scan for one or two beams takes about 30 to 60 seconds.

The mechanism of signal formation can best be understood if one calculates the fields set up by the beam. We therefore proceed to this calculation and to this end we first describe the characteristics of the SPEAR beam.

The SPEAR Beam and Its Fields

The main parameters of the storage ring are found in ref. 1. Each beam is composed of a short bunch of particles revolving at the frequency $F_0 = 1.28$ MHz.

The charge distribution is very nearly Gaussian in the longitudinal direction, and approximates a delta function in the transverse dimensions. For practical purposes we can write:

$$\lambda(z,t) = \lambda_0 e^{-\frac{(z - vt)^2}{2\sigma^2}}$$

$$\lambda_0 = i_0/\sigma\sqrt{2\pi}\ F_0$$

where λ is the linear charge density, σ is the longitudinal half bunch width, v is the particle's velocity and i_0 is the average beam current. To calculate the fields set up by $\lambda(z,t)$ it is convenient to carry out the analysis in the beam system of reference which moves at velocity v in the z direction. (See ref. 2.) Then the charge distribution λ and the current density J_z on one hand, and the longitudinal coordinate z and time t on the other hand, transform into λ', J_z', z', t' in the new frame of reference, in the following way:

$$\begin{Bmatrix} J_z \\ i\lambda \end{Bmatrix} = \begin{bmatrix} \gamma & -i\beta\gamma \\ i\beta\gamma & \gamma \end{bmatrix} \begin{Bmatrix} J_z' \\ i\lambda' \end{Bmatrix} \qquad \begin{Bmatrix} z \\ ict \end{Bmatrix} = \begin{bmatrix} \gamma & -i\beta\gamma \\ i\beta\gamma & \gamma \end{bmatrix} \begin{Bmatrix} z' \\ ict' \end{Bmatrix} \tag{2}$$

with $i = \sqrt{-1}$ $\quad \beta = \frac{v}{c}$ $\quad \gamma = (1 - \beta^2)^{-1}$

However we note that $J_z' = 0$ since there is no movement of charge in the beam system of reference, and (1) becomes:

$$\lambda'(z') = \frac{\lambda_0}{\gamma} e^{-\frac{z'^2}{2\sigma'^2}} \tag{3}$$

with $\sigma' = \gamma\sigma$.

So for $v \to c$ the effect of the Lorentz transformation is to spread the charge over an infinitely long line charge, without altering the transverse dimensions. If E' and B' are the fields due to λ', then from (2), the transverse components E_T and B_T in the laboratory system of reference are given by:

$$\begin{aligned} E_T &= \gamma \left(E'_T - \frac{v}{c} \times B'\right) \\ B_T &= \gamma \left(B'_T + \frac{v}{c} \times E'\right) \end{aligned} \tag{4}$$

and since $B' = 0$ we simply have

$$\begin{aligned} E_T &= \gamma E'_T \\ B_T &= \gamma \frac{v}{c} \times E' \end{aligned} \tag{5}$$

that is, the calculation of the electric field only, yields both electric and magnetic fields, and for $v \approx c$, these fields turn out to be equal, (C. G. S. units).

Electric Field

The problem of the position monitor is thus reduced to the calculation of the electric field due to a line charge parallel to the axis of a circular cylinder which, we will assume, has infinite conductivity.

In the general case the line charge is not at the center of the cylinder (Fig. 1). The method of images can be used to express a potential function ϕ', and then E' can be derived as the gradient of ϕ'. At the walls E' reduces

to its normal component E'_n, and transforming back to the laboratory system of coordinates we get: (practical units)

$$E_n = \frac{\lambda(z,t)}{2\pi\epsilon_0 a} F(\delta,\theta)$$

$$H_t = \sqrt{\frac{\epsilon_0}{\mu_0}}\, E_n \qquad (6)$$

$$F(\delta,\theta) = \frac{a^2 - \delta^2}{a^2 + \delta^2 - 2a\delta \cos\theta}$$

with a the cylinder radius, and δ, θ the beam position in polar coordinates.

We recognize the first factor of E_n as the beam current dependent term, and the function $F(\delta, \theta)$ as the beam position dependent term.

Monitor Equivalent Circuit

At this point, we may choose to build a monitor which samples the electric field, or a monitor which samples the magnetic field. As far as the position sensitivity is concerned, it will be identical for both types since $F(\delta, \theta)$ appears in the same way in E_n and H_t. However, the two circuits are not quite the dual of each other when it comes to their sensitivity to beam current.

For an electrostatic type of monitor we calculate from E_n the charge q on the electrode, and the equivalent circuit (Fig. 2) is a current source dq/dt driving a parallel RC impedance, where C is the electrode capacity.

For the magnetic type, which uses loops instead of electrodes, the equivalent circuit is a voltage source $d\phi/dt$, ϕ being the flux through the loop, driving a series LR impedance, where L is the loop self inductance. In both cases R is the external load and in most practical situations R = 50 Ohms.

When comparing a small electrode of say 1 inch diameter, to a small loop of the same dimension, it turns out that in the first case $\omega RC \ll 1$ for the most significant beam waveform frequencies, and in the second case $\omega L/R \ll 1$. Therefore, the electrode voltage will be $V_e = R\, dq/dt$, whereas the loop voltage will be

$$V_m = d\phi/dt = \frac{1}{R}\sqrt{\frac{\mu_0}{\epsilon_0}}\ V_e \approx 7.5\ V_e.$$

This advantage might be thought to be a decisive point in favor of loops. However, for a positron-electron storage ring it is convenient to be able to identify the beams at each monitor station, and only the electrostatic monitor can provide this information since the polarity of its signals is the same as that of the beams. Fig. 3 shows the two SPEAR beams as they appear out of one monitor electrode; the monitor is situated at approximately 12 meters from the beams' crossing point.

From (6) the charge on one electrode of diameter d, located at $z = 0$, is found to be:

$$q = \pi\frac{d^2}{4}\,\epsilon_0 E_n\Big|_{z=0} = \frac{d^2}{8a}\ F(\delta,\theta)\ \lambda_0 e^{-\frac{c^2t^2}{2\delta^2}} \qquad (7)$$

The exponential function has the extrema of its derivative at $t = \pm\sigma/c$. From now on we will refer to "electrode voltage" as the amplitude of one

of the extrema of R dq/dt, as observed at each of four electrodes A, B, C and D in a 45° configuration (Fig. 4):

$$V_{A,B,C,D}(\lambda_0,\sigma,\theta) = R\frac{d^2}{8a}\frac{c\lambda_0}{\delta\sqrt{e}}F(\sigma,\theta) \qquad \theta = \frac{3\pi}{4},\frac{\pi}{4},-\frac{\pi}{4},-\frac{3\pi}{4} \tag{8}$$

for $\sigma \approx 0$. $F(\sigma,\theta)$ is unity and with (1) we get

$$V_{A,B,C,D}(i_0) = R\frac{d^2}{8a}\frac{c\,i_0}{\delta^2\sqrt{2\pi e}\,F_0} \tag{9}$$

For $i_0 = 1$ mA average, R = 50 Ohms, d = 2.54 cm, a = 10 cm and δ = 14 cm, we have $V_{A,B,C,D} = 115$ mV/mA average. This figure was deemed to be acceptable, 1 mA being the lowest beam current at which the machine studies are usually carried out.

Calibration Factor -- Pin Cushion Distortion

We have found that each electrode voltage $V_{A,B,C,D}$ was proportional to the beam current and to a function $F(\delta,\theta)$ of the beam position with respect to each electrode.

From Figure 4 we recognize that the beam position is given by:

$$x = \frac{-V_A + V_B + V_C - V_D}{V_A + V_B + V_C + V_D}K_x(x,y)$$

$$y = \frac{V_A + V_B - V_C - V_D}{V_A + V_B + V_C + V_D}K_y(x,y) \tag{10}$$

where K_x and K_y are geometric factors which we call "monitor calibration

factors," and which have the dimension of length. It is more convenient at this point to assign Cartesian coordinates to the beam, and to perform the following substitution (Fig. 1):

$$\delta = \sqrt{x^2 + y^2}$$

$$\theta_{A,B,C,D} = n\frac{\pi}{4} - \tan^{-1}\frac{y}{x} \qquad n = 3,1,7,5$$

Four functions $F_A(x,y)$, $F_B(x,y)$, $F_C(x,y)$ and $F_D(x,y)$ result, and substituting equation (8) into (10) we have:

$$x = \frac{-F_A + F_B + F_C - F_D}{F_A + F_B + F_C + F_D} K_x(x,y)$$

$$y = \frac{F_A + F_B - F_C - F_D}{F_A + F_B + F_C + F_D} K_y(x,y) \qquad (11)$$

with $F_{A,B,C,D} = (a^2 - x^2 - y^2)\left[a^2 + x^2 + y^2 - 2a\sqrt{x^2 + y^2}\,\mathrm{Cos}\left(n\frac{\pi}{4} - \tan^{-1}\frac{y}{x}\right)\right]^{-1}$

and n= 3, 1, 7, 5.

Now we can calculate $K_x(x,y)$ and $K_y(x,y)$ using (11). At the origin a limit can be obtained and we get

$$K_x(0,0) = \frac{a}{\sqrt{2}} \qquad (12)$$

On Figure 5 we plot the relative value of the calibration factors when the beam position assumes coordinates confined to a 0 - 2.8 cm square. In other words, the plot of Figure 5 represents the monitor response, should a constant calibration factor $a/\sqrt{2}$ be used.

Laboratory Measurement of the Calibration Factors

In the above calculation we have neglected the field distortion created by the proximity of the synchrotron radiation masks (Fig. 4). These water cooled masks are required to protect the straight sections' vacuum chamber walls from the synchrotron radiation. Each monitor is associated with a mask, and the transverse symmetry of the structure has been restored by installing a dummy mask on the opposite side.

The measurements of the calibration factors were carried out in the laboratory, by sending a current pulse on a rod parallel to the monitor axis. Note that the pulse shape is unimportant since expression (11) for K_x and K_y does not include current dependent terms.

The four electrode voltages were measured with a sampling oscilloscope, as the rod was moved along the horizontal or the vertical axes. The measured plots of Fig. (6) are simply the variation of the expression

$$K_{\substack{x \\ y}} = \frac{V_A + V_B + V_C + V_D}{\pm V_a + V_B \pm V_C - V_D} \quad \begin{matrix} x \\ y \end{matrix}$$

and the calculated curve is a representation of equations (11) and (12). We observe different sensitivities in the vertical and horizontal direction, due most likely to the radiation masks, and better agreement with the calculation when the rod is off center. It was felt that a single value for K_x and K_y could be picked which would be satisfactory for all beam positions up to ± 2 cm, and since the error introduced by the masks is considerably more significant than the pin cushion distortion, the latter has been discarded. The calibration factor adopted for the SPEAR position monitors is $K_x = K_y = 70$ mm.

Processing Factors

We turn now to the circuit used to derive an analog signal proportional to the electrode peak voltage. The bipolar pulses of Fig. 3 are integrated. The transfer function of the integrator (Fig. 7) is:

$$V_{out} = \frac{\alpha}{RC} \int V_{in}\, dt$$

where α is the transistor current transfer ratio, R the cable termination resistor, and C is the transistor's collector-base capacity and the stray capacity. Fig. 8 shows a typical integrator input-output waveform. Beyond the integrator, two identical circuits, one for each beam, comprise a Darlington pair, a 6 diode series linear gate, a dc restorer, a peak detector and an operational amplifier.

The response of this circuit has been measured for each beam, as a function of one electrode voltage or rather as a function of each beam current (Fig. 9). One might think that the nonlinearity of the curve and its ordinate at the origin are unimportant, since the beam poisition measuring process requires taking the difference between two such signals. However, the current normalization as epxressed by equation (10) involves summations too, and we found a strong dependency of the measured orbits on the beam current. After attempting to build a more linear peak detector, it was decided that this endeavor was doomed to failure because of the narrowness of the electrodes' pulses, and that the linearization of the data could be easily programmed out during the computer orbit calculations.

Position Scanning (General)

Physical lengths of coaxial cable between control-room processing electronics and position-monitor pickup electrode are as long as 130 meters. As shown in Fig. 3, the voltage pulse produced by an electrode is quite narrow (1 nsec). To insure pulse fidelity, coaxial relays are required for switching and 7/8-inch-diameter heliax is used for the cable run.

The ring is split into four quadrants with five position monitor stations per quadrant. These five positions are multiplexed with coaxial relays onto four heliax cables to the control room. The four cables carry electrode signals of the position addressed in that quadrant. At the control room, sixteen heliax cables contain signals from four pick-up electrodes of twenty position monitors; these are again multiplexed with coaxial relays to one cable and sent to the processing electronics. Cable lengths to each quadrant have been matched, and electrode signals of any position are delayed equally to within 1 nsec.

Electrode-signal monitor points, ahead of processing electronics are available and have been very useful during beam-stability analysis when displayed on a fast real-time oscilloscope. Manual and automatic attenuation of the electrode signals are provided in order to maintain levels within the range of the processing electronics. Beam current intensity data is used as an input to an A/D converter to automatically insert 6 dB steps of attentuation in addition to the manual attenuation which may be switched in.

Electrode signals are processed serially in the following sequence. Computer on - - - - read e^+ offset voltage - - - - read e^- offset voltage - - - - first position, electrode A read e^+ voltage minus e^+ offset - - - - read e^- voltage

minus e^- offset - - - -same position electrode B - - - -read e^+ voltage minus e^+ offset - - - -read e^- voltage minus e^- offset. Twenty positions are read by the computer in this manner with a full scan taking 30 to 60 seconds to complete. e^+ and e^- signals are separated in the Signal Processing circuit by gating techniques with a positive dc voltage appearing at the e^+ output and a negative dc voltage appearing at the e^- output. These outputs branch off to the computer interface and a front panel DVM located on the position-monitor control panel.

Scanning Electronics

Since each monitor station has a unique time relationship with reference to a main trigger, position selection is used as an "address" input to a precise and electronically variable trigger-delay generator. These triggers are variable in 5-nsec increments and are used as gate generator inputs to the Signal Processing module. Delayed triggers are also available as oscilloscope triggers when monitoring electrode signals.

The entire process is controlled by the SPEAR computer in a seven-bit binary word plus one strobe (S_1) and one control line (C_0). Electronics of the system are housed in three rack-mounted cassis. POSITION MONITOR CONTROL chassis is located at the operator console, with the remaining two units in a remote rack. Design is such that a complete orbit, consisting of twenty monitors may be scanned in any sequence desired.

Manual selection of position and electrode with readout on a DC digital voltmeter (DVM) is provided with push-button switches at the control panel. Manual operation is disabled when the computer comes on-line (C_0 true) and must be re-selected after automatic scanning is complete. A high frequency

oscilloscope is used to monitor electrode signals prior to the analog circuitry. Lamps in the push-button switches indicate position and electrode selection in both automatic and manual modes.

Scanning Operation

Bipolar signals from MONITOR pickup electrodes are delivered to the SPEAR control room via 7/8" heliax cables. Four quadrants of four cables per quadrant carry electrode signals (A, B, C, D) selected from one of five monitors in that quadrant.

When automatic scan is desired, C_0 goes true (High) and stays high throughout the complete orbit -scanning process. Any manual select switches which were "on" are disabled; programmable attentuators are held in their last state of attneuation, and the position/electrode binary decoder is enabled. Five bits of a seven-bit word are used to select 1 of 20 position locations around the ring, with the remaining two bits of the word for A, B, C, D electrode selection. Strobe S_1, which is normally high during auto scan, goes to LO only during address changes; this is used to inhibit the decoders during address changes.

Selection of a monitor position activates eight coaxial relays of that monitor which apply four electrode signals to the four cables of the quadrant; also, the proper quadrant relays are activated by using position information as inputs to a five-input "OR" circuit. Position selection is also used as an input to a 20×16 pin programmable matrix. Eight of the matrix outputs are used for the e^+ trigger delay circuit and eight are used for e^- delay circuits.

All logic circuitry described uses T^2L integrated circuits. Power transistors are used as coaxial relay drivers. Efforts have been made to eliminate

ground loops by using opto-isolators between the computer and position control chassis, and twisted pair wires between relay drivers and floating relay coils.

Trigger Delay Generator

A trigger delay unit described herein uses Motorola Emitter Coupled Logic (MECL) integrated circuits. A new series of logic elements (MECL 10,000) is used extensively in this design. These elements have typical gate delays of 2 nsec, which places their speed between MECL II and MECL III. Maximum toggle frequency of a type "D" flip-flop is specified as 150 MHz, which is well over our design criteria of 102 MHz. This circuit uses seven stages of type "D" flip-flops in a ripple counter configuration, and operates at a frequency which corresponds to the desired delay increments. Outputs from the flip-flops are used as inputs to EXCLUSIVE-OR comparators, then "AND"-ed down the line to a final output.

Referring to Fig. 12, circuit operation is as follows: A NIM trigger input at the ring revolution frequency of 1.28 MHz is level shifted, shaped and applied to all FF reset lines through gates used as delay elements.

A 102-MHz clock, which is derived from the ring rf frequency of 51 MHz and phase synchronized to the 1.28 MHz, is level shifted and applied to the first flip-flop. This frequency division which is now a 20 nsec period (10 nsec Hi - 10 nsec Lo) is an input to the first "EX-OR." Active delay increments are 10 nsec, with a 50-ohm cable used as a 5-nsec delay. Assuming the fifth pulse of Fig. 12 is desired at the output, and address of (2^3 Hi - 2^2 Lo - 2^1 Hi) will allow only the pulse in time slot 5 through the series of "AND" gates. Understanding the circuit concept will immediately disclose the need for accurate timing between the ripple counter and gate delays. Although not indicated

in Fig. 12, there are delay gates used between "EX-OR", "AND", and "FLIP-FLOPS." Theoretically, the circuit as described could be used to ripple a 5-nsec pulse through by using the clock as an input to the first comparator. Reasons for avoiding this approach are (1) pushing the I.C. gates to their full rise - falltime capabilities; (2) our requirement of the circuit to reset and be ready within a clock period.

Addressing of the delay generator is in straight binary and is programmed with a pin matrix. Output is fanned out to four NIM levels, 10 nsec wide. Delay variations are dependent only on clock stability, which in this case is the ring rf stability. Circuit propagation delay is 50 nsec and the maximum usable delay is 50 nsec ÷ 830 nsec.

Digital delay units using this concept are used throughout the SPEAR experimental area as a convenient method of obtaining synchronized, variable delayed triggers. One problem with this system is the requirement of short term and long term phase stability between the 1.28 MHz reset pulse and 102 MHz clock. A drift of ± 5 nsec will force the counter to try clocking and reseting at the same instant. The result is a delayed output pulse which will jump 10 nsec as the flip-flops decide which will win the race between clock and reset. This problem has been attacked by building a frequency synthesizer, using phase locked loop design, to provide various stable frequencies required by the ring.

Acknowledgements

The authors wish to thank Burt Richter and J. R. Rees for specifying and patiently evaluating this system, and all the members of the storate ring group who participated at one time or another in orbit measurements. One of us (J.-L. P.) is indebted to Phil L. Morton for the fruits of many interesting conversations. It is also a pleasure to thank R. A. Scholl for his thorough contributions to all phases of this project, as well as A. M. Boyarski and Alex King for programming the beam orbit calculations. The mechanical design of the monitors and their alignment is due to L. G. Karvonen.

REFERENCES

1. SLAC Storage Ring Group, Proc. CERN Symposium on High Energy Accelerators, 1971.
2. Melvin Schwartz, Principles of Electrodynamics (McGraw Hill, New York, 1972).

FIGURE CAPTIONS

1. Coordinate systems for fields and distortion calculations.
2. Equivalent circuit of a) electrostatic position monitor; b) magnetic position monitor.
3. Electrode waveform for a monitor located 12 meters from the beams' crossing point. 0.1 volt/div., 20 nsec/div.; total average beam current, 14 mA.
4. Position monitor geometry.
5. Calculated monitor response to linear beam displacements assuming $K_x(x,y) = K_y(x,y) = K_x(0,0) = 100 \text{ mm}/\sqrt{2}$.
6. Calibration factor as a function of beam position on the vertical or the horizontal axes.
7. Position monitor processing electronics. Partial schema.
8. Integrator waveform. Lower trace: input, 1 volt, 2 nsec. Upper trace: output, 0.5 volt, 2 nsec.
9. Beam position monitors. Processing electronics' response as a function of average beam current.
10. General location of position monitor stations and cable run.
11. Block diagram of position monitor scanning electronics.
12. Block diagram of digital delay unit.
13. Position monitor control chassis.
14. Relay driver and trigger delay.
15. Relay chassis.

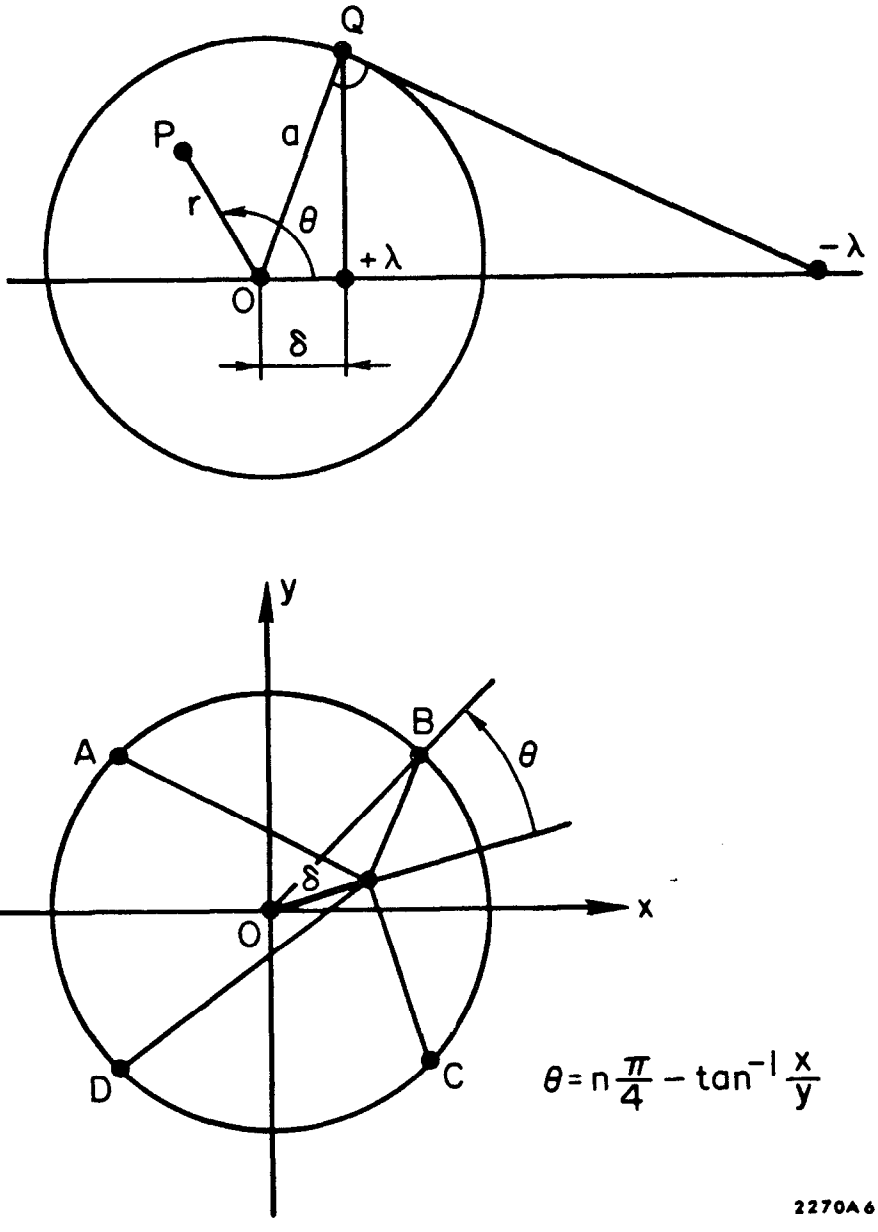

FIG. 1

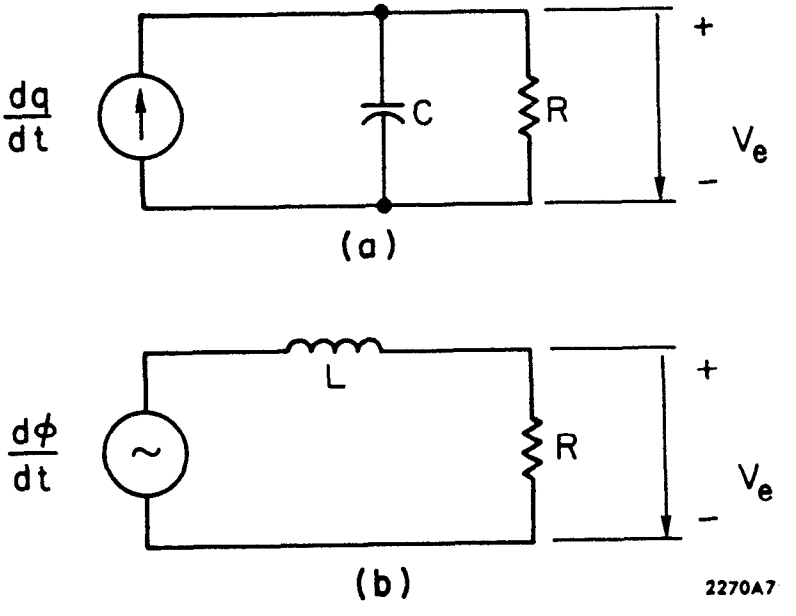

FIG. 2

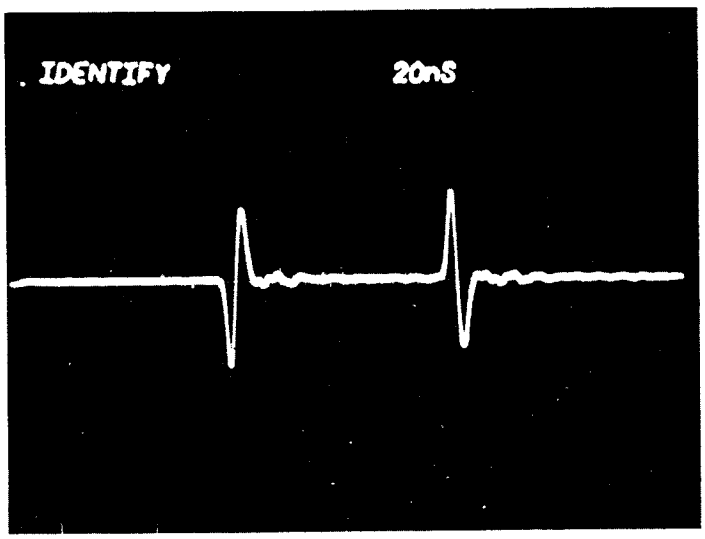

2270A8

FIG. 3

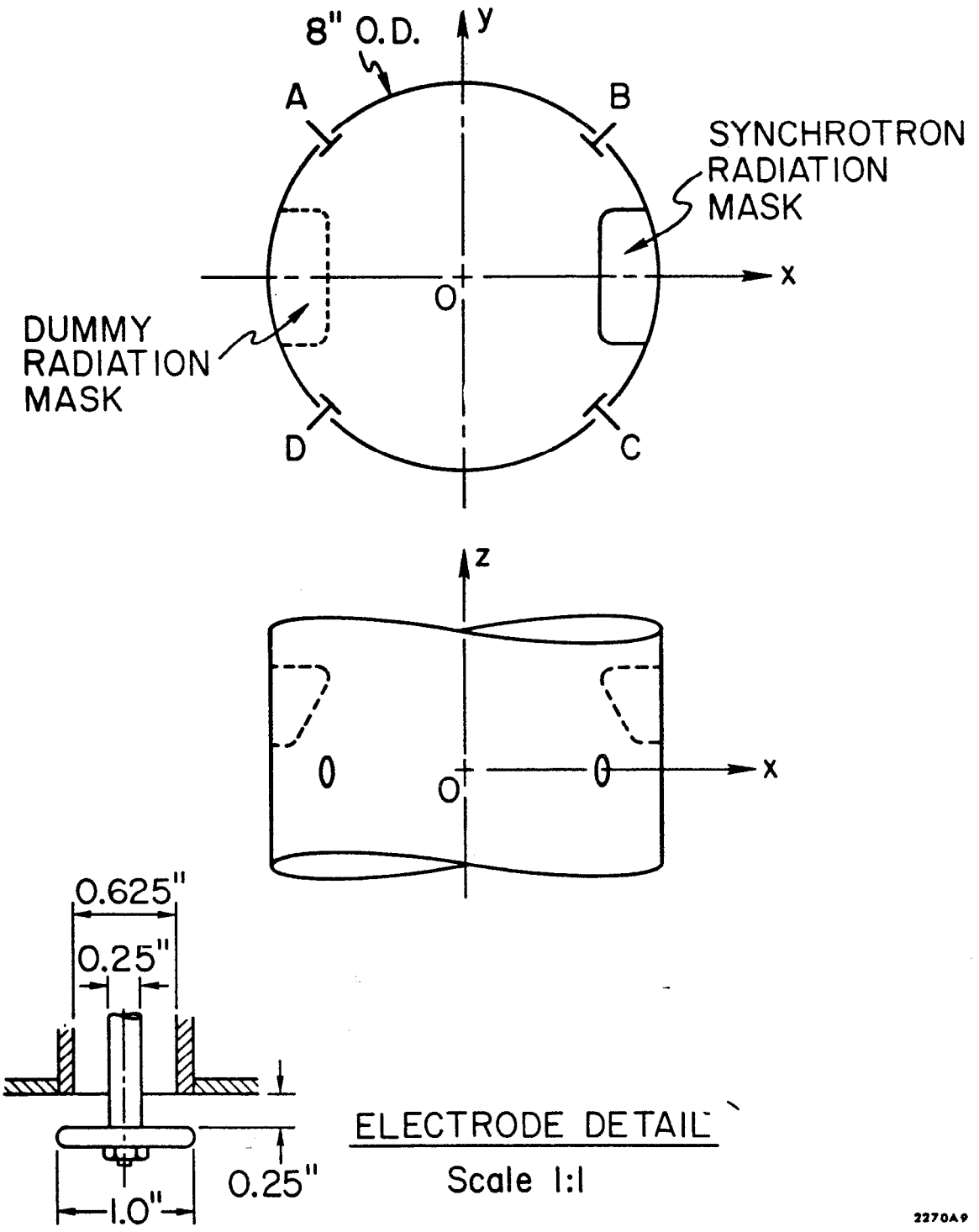
8" O.D.
y
A
B
SYNCHROTRON
RADIATION
MASK
x
O
DUMMY
RADIATION
MASK
D
C
z
0
0
0
x
0.625"
0.25"
0.25"
1.0"
ELECTRODE DETAIL
Scale 1:1
2270A9

FIG. 4

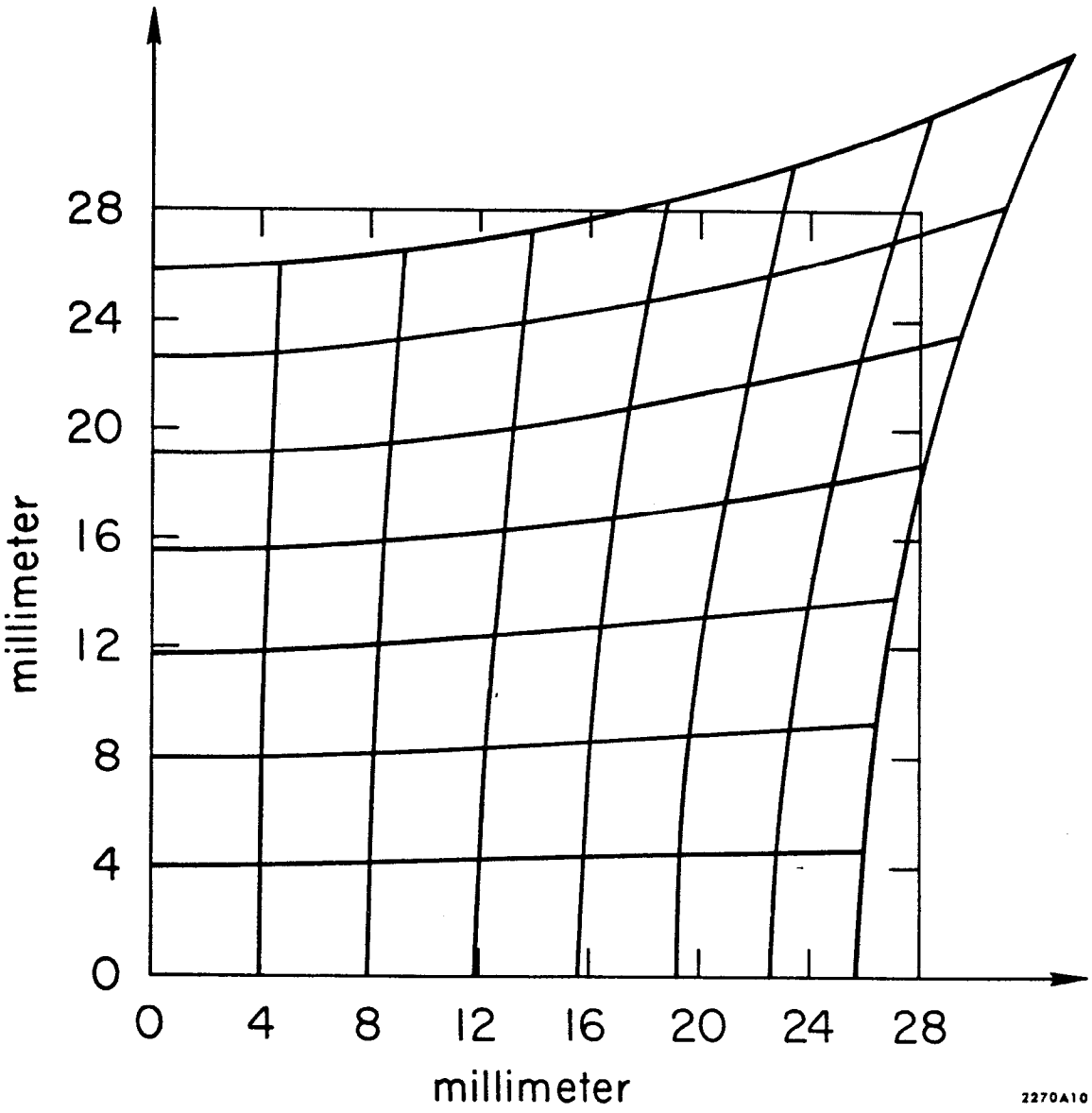
28
24
20
16
12
8
4
0
millimeter
0
4
8
12
16
20
24
28
millimeter
2270A10

FIG. 5

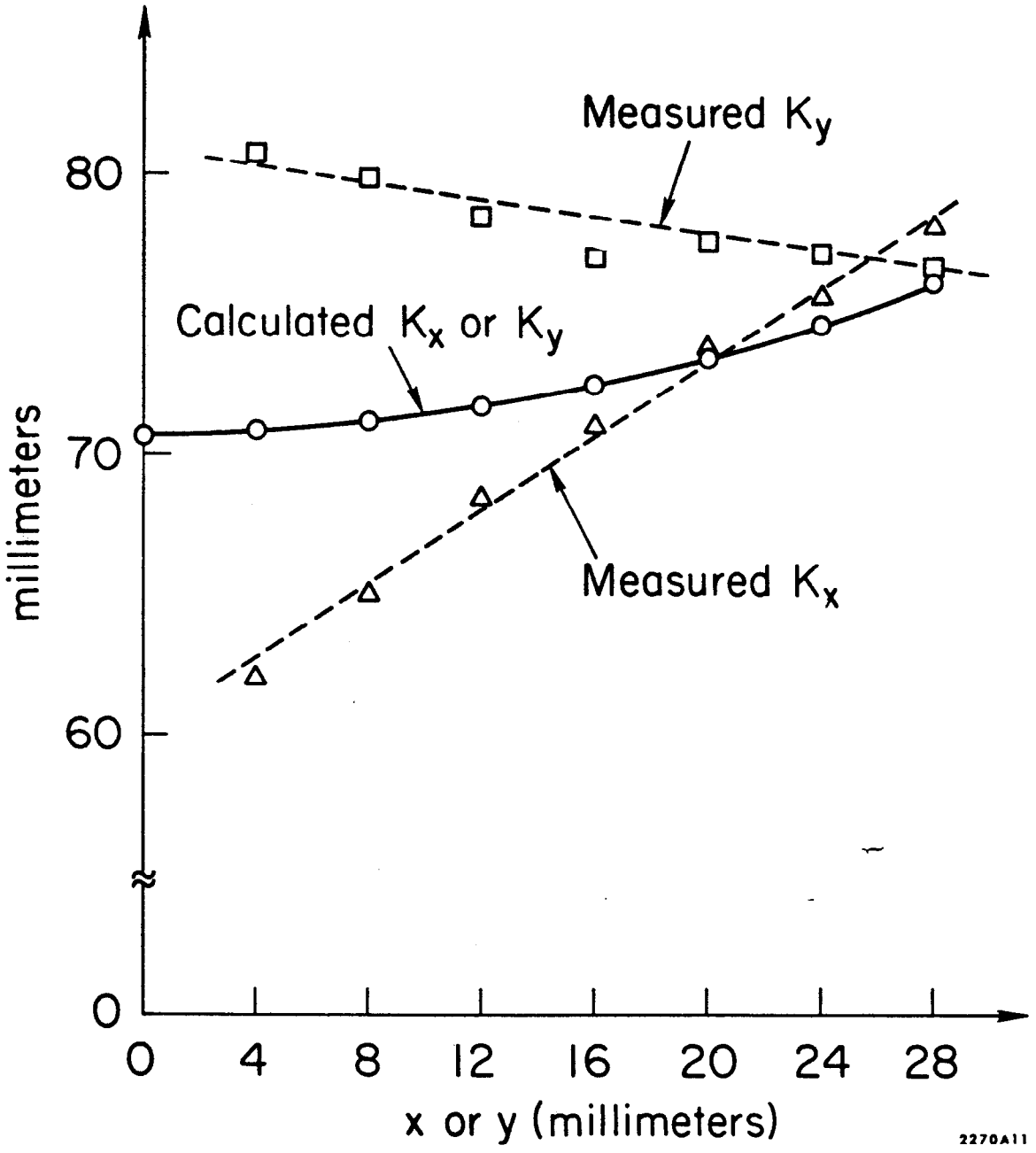
Measured K_y
Calculated K_x or K_y
Measured K_x
millimeters
80
70
60
0
0
4
8
12
16
20
24
28
x or y (millimeters)
2270A11

FIG. 6

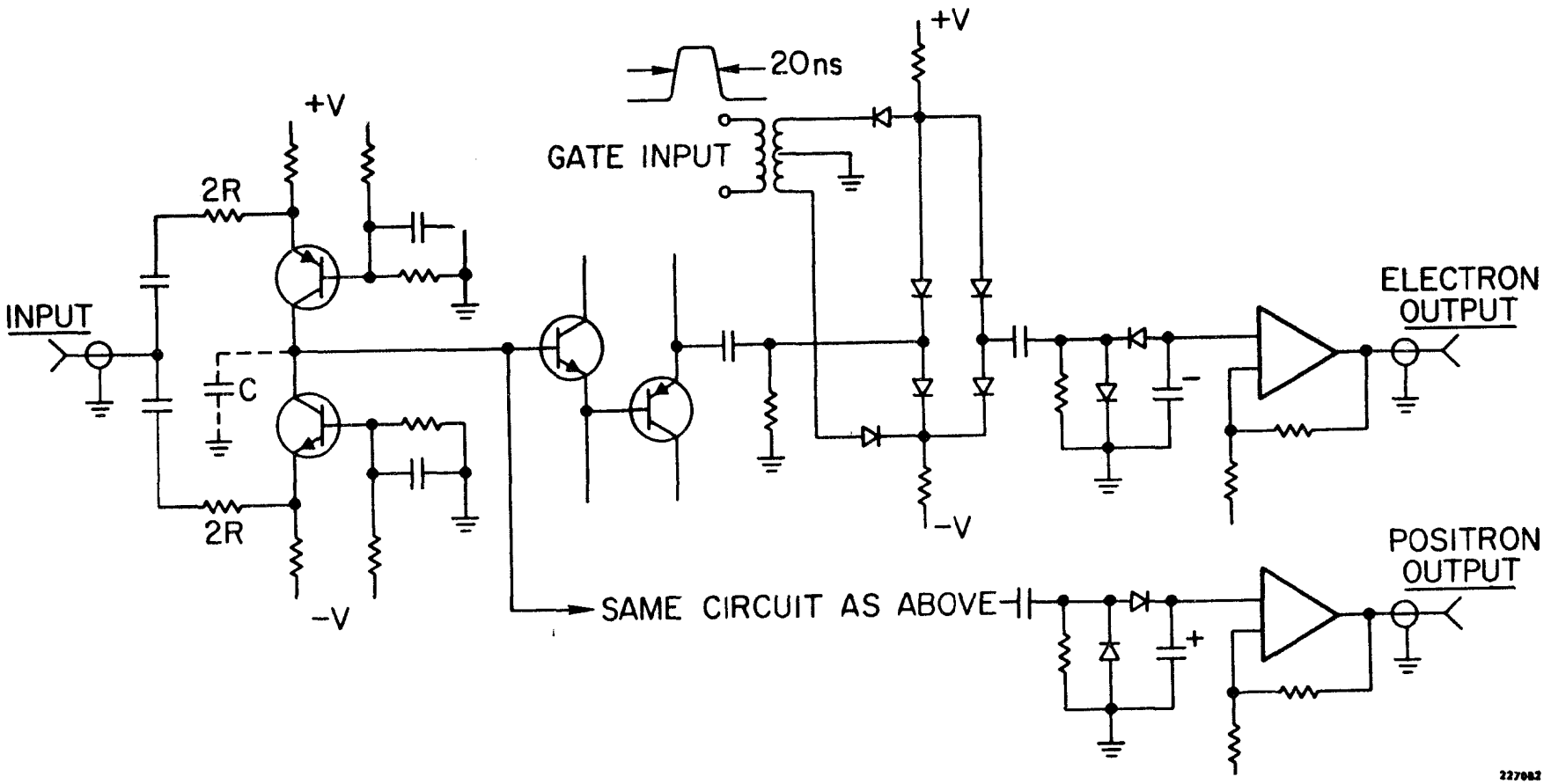
+V
20ns
GATE INPUT
+V
2R
INPUT
C
2R
-V
-V
ELECTRON
OUTPUT
POSITRON
OUTPUT
SAME CIRCUIT AS ABOVE
227082

FIG. 7

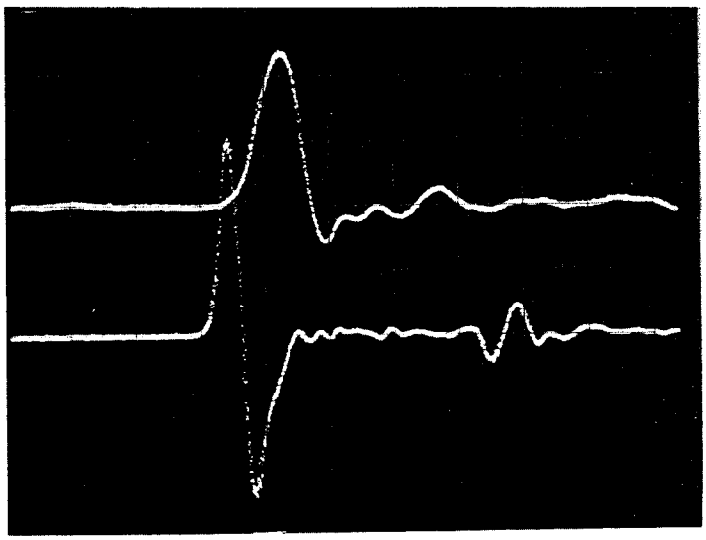

2270A12

FIG. 8

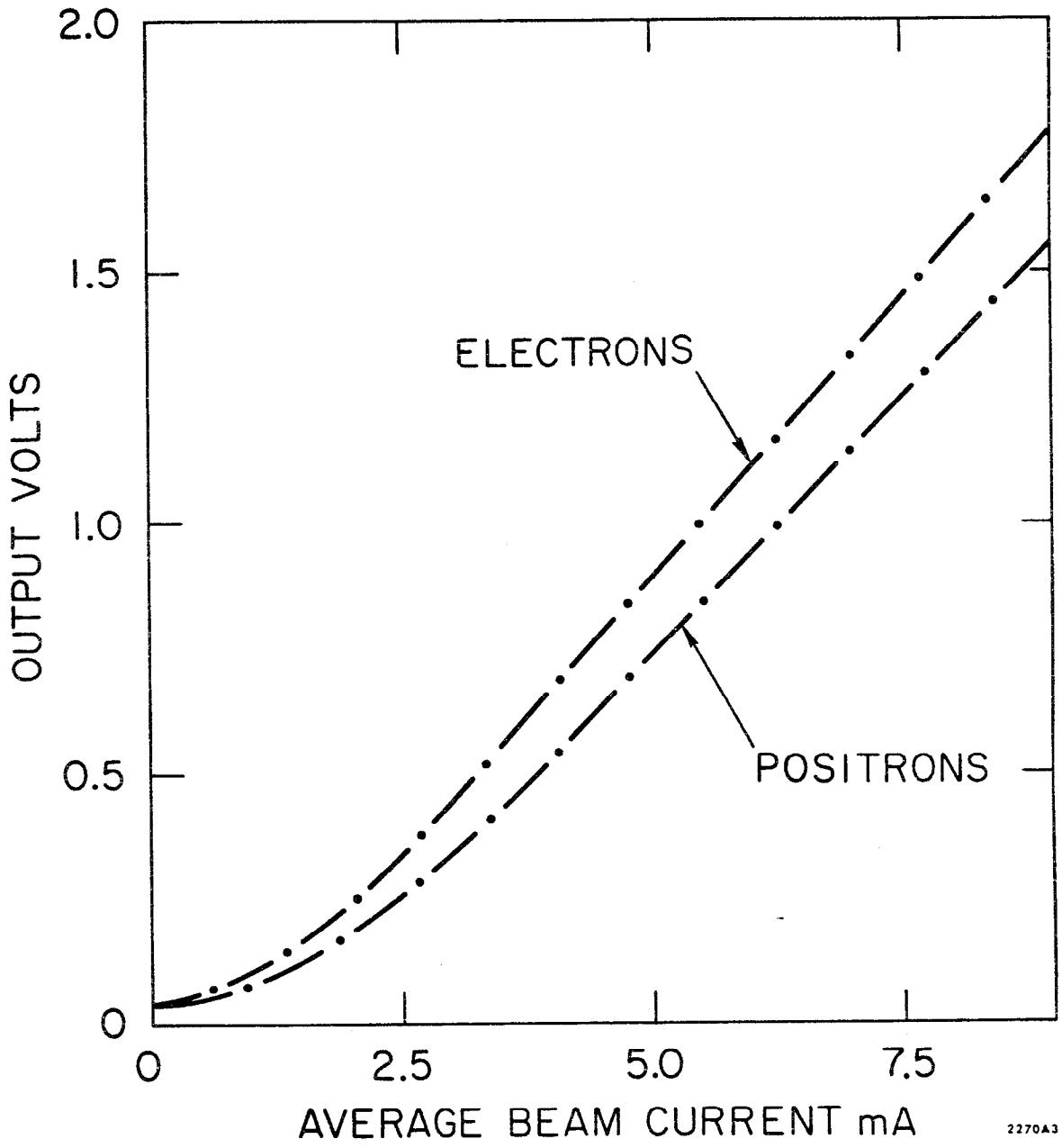
2.0
1.5
1.0
0.5
0
OUTPUT VOLTS
ELECTRONS
POSITRONS
0
2.5
5.0
7.5
AVERAGE BEAM CURRENT mA
2270A3

FIG. 9

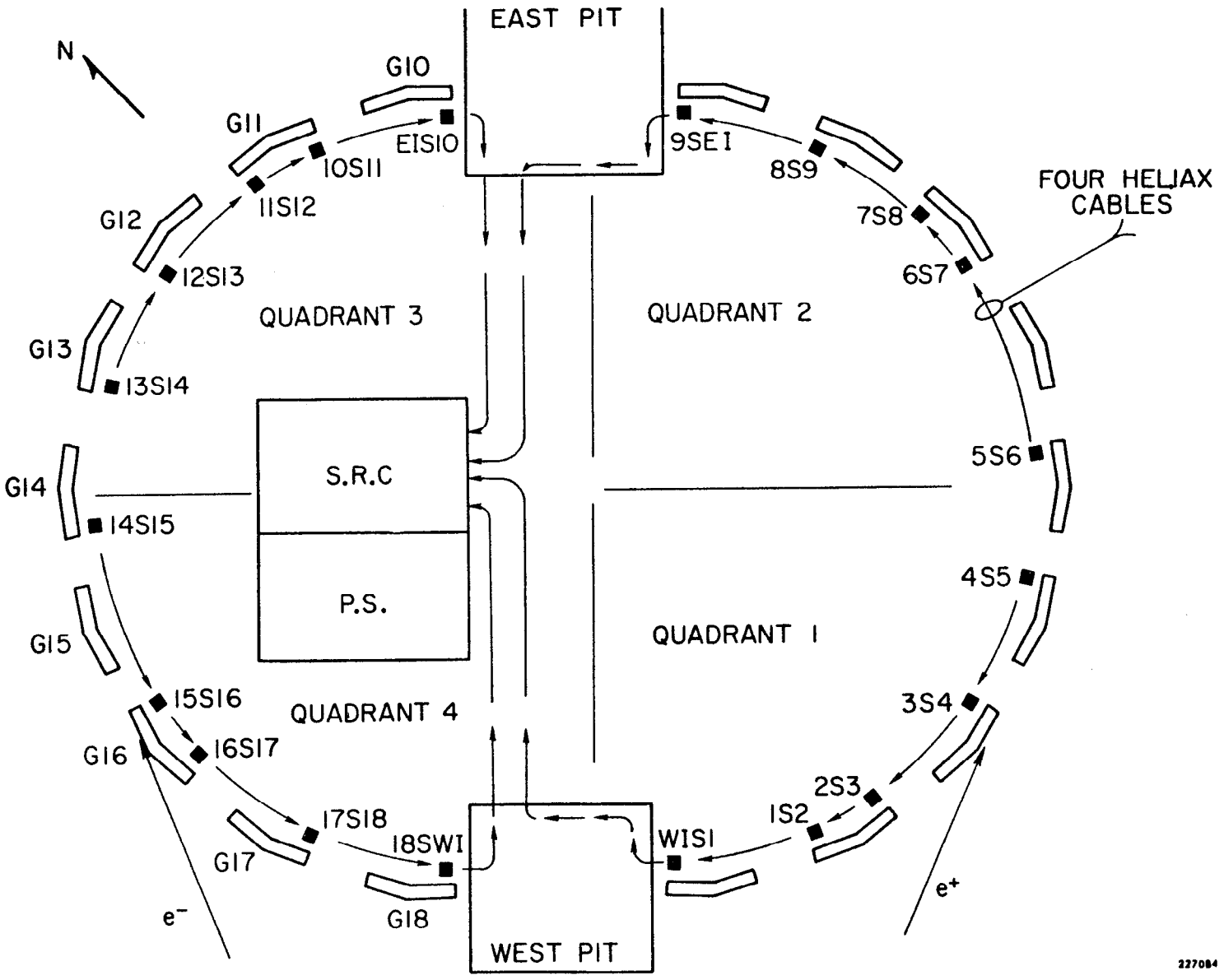
EAST PIT
N
G10
G11
EIS10
10S11
9SE1
8S9
FOUR HELIAX CABLES
7S8
G12
11S12
6S7
12S13
QUADRANT 3
QUADRANT 2
G13
13S14
S.R.C
5S6
G14
14S15
P.S.
4S5
G15
QUADRANT 1
15S16
QUADRANT 4
3S4
G16
16S17
2S3
17S18
1S2
18SWI
WIS1
G17
e⁻
G18
e⁺
WEST PIT
227084

FIG. 10

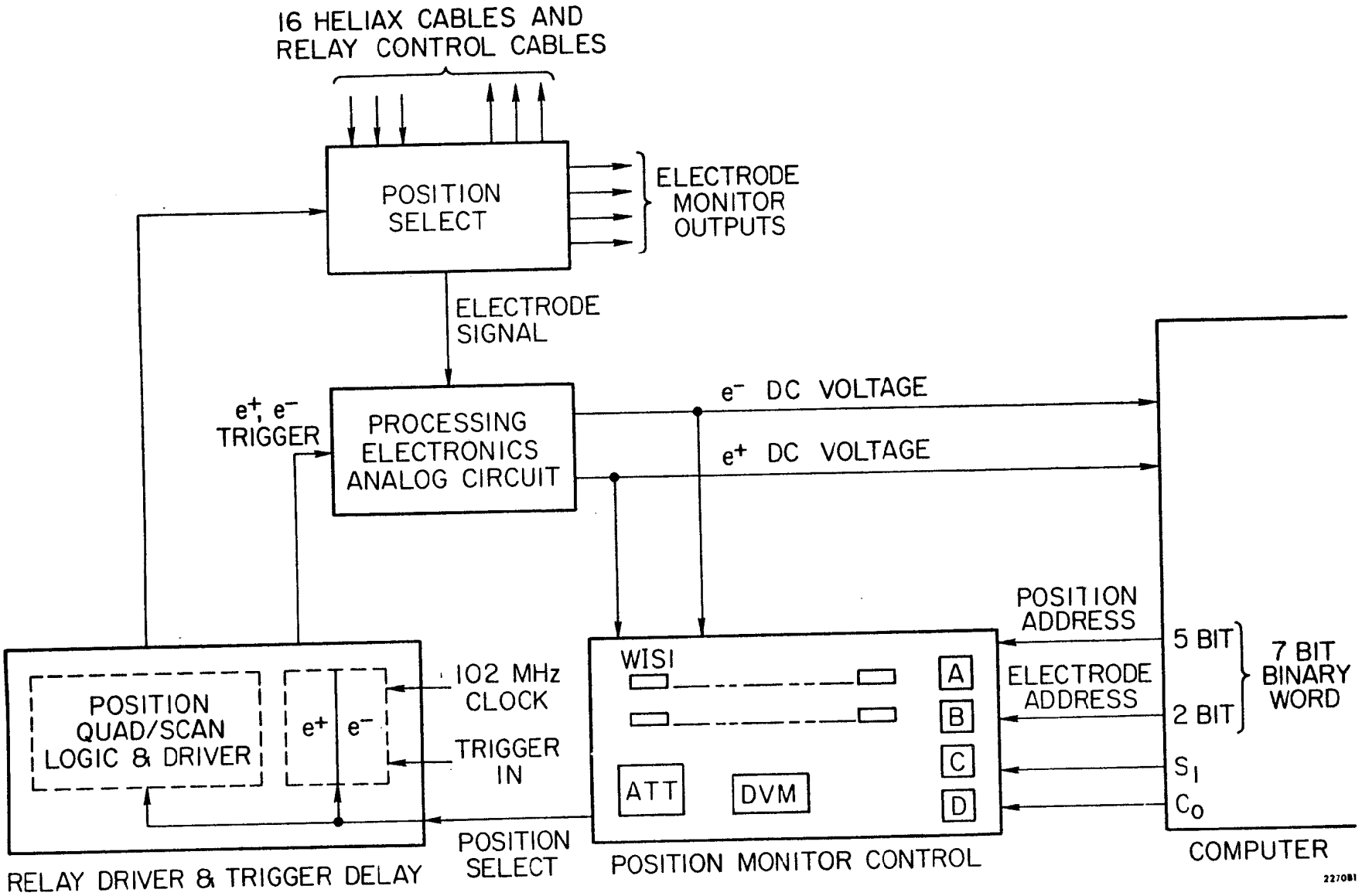
16 HELIAX CABLES AND
RELAY CONTROL CABLES
POSITION
SELECT
ELECTRODE
MONITOR
OUTPUTS
ELECTRODE
SIGNAL
e+, e−
TRIGGER
PROCESSING
ELECTRONICS
ANALOG CIRCUIT
e− DC VOLTAGE
e+ DC VOLTAGE
POSITION
ADDRESS
5 BIT
7 BIT
BINARY
WORD
2 BIT
ELECTRODE
ADDRESS
WISI
A
B
C
D
ATT
DVM
S1
Co
COMPUTER
POSITION
QUAD/SCAN
LOGIC & DRIVER
e+
e−
102 MHz
CLOCK
TRIGGER
IN
POSITION
SELECT
RELAY DRIVER & TRIGGER DELAY
POSITION MONITOR CONTROL
227081

FIG. 11

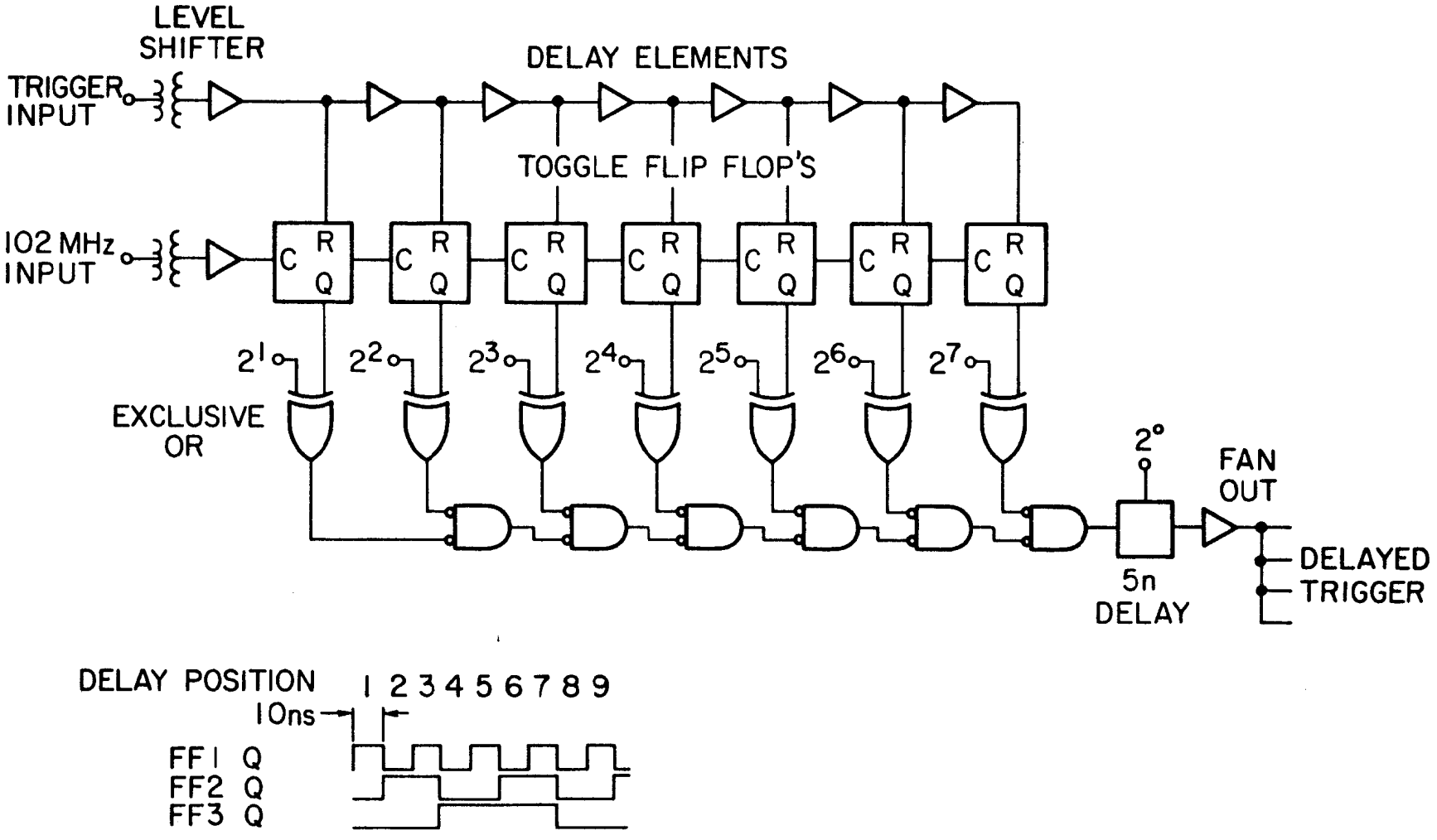
LEVEL
SHIFTER
DELAY ELEMENTS
TRIGGER
INPUT
TOGGLE FLIP FLOP'S
102 MHz
INPUT
C R
Q
2^1
2^2
2^3
2^4
2^5
2^6
2^7
EXCLUSIVE
OR
2^0
FAN
OUT
DELAYED
TRIGGER
5n
DELAY
DELAY POSITION 1 2 3 4 5 6 7 8 9
10ns
FF1 Q
FF2 Q
FF3 Q

FIG. 12

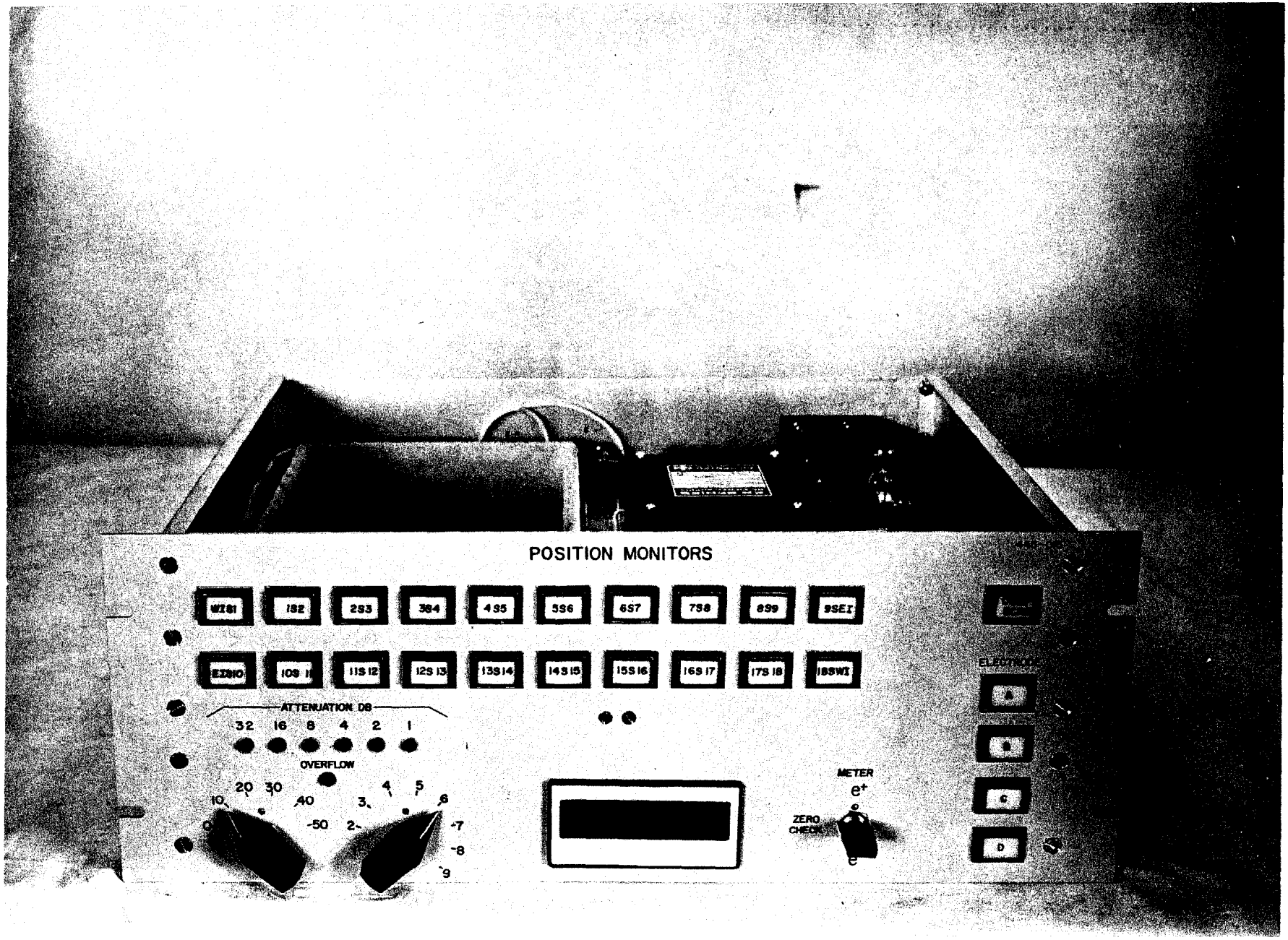
POSITION MONITORS
WIS1
1S2
2S3
3S4
4S5
5S6
6S7
7S8
8S9
9SE1
E1SW0
10S 11
11S 12
12S 13
13S 14
14S 15
15S 16
16S 17
17S 18
18SW1
ATTENUATION DB
32 16 8 4 2 1
OVERFLOW
10 20 30 40 -50
1 2 3 4 5 6 -7 -8 -9
METER
e+
e-
ZERO
CHECK
C
D

FIG. 13

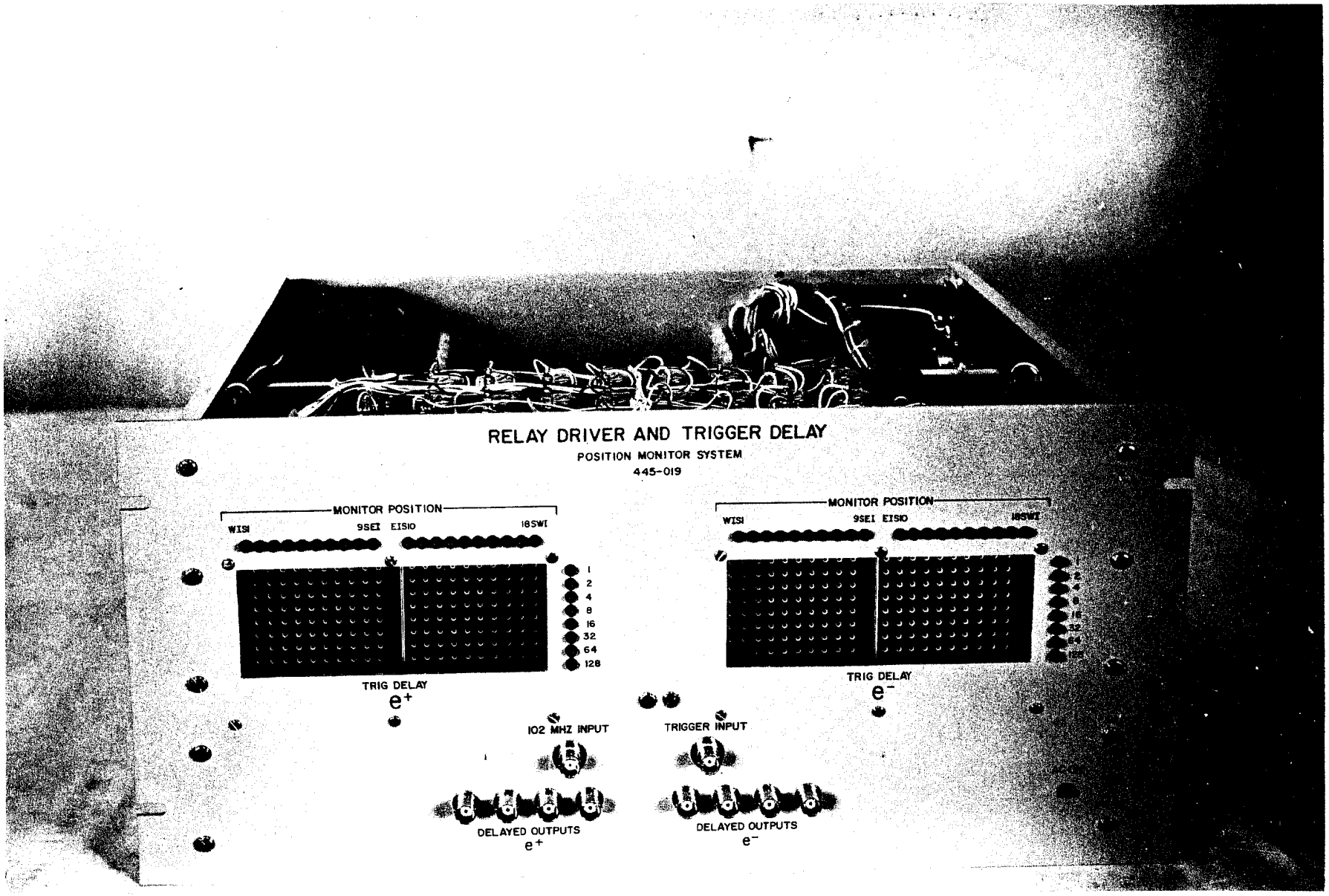
RELAY DRIVER AND TRIGGER DELAY
POSITION MONITOR SYSTEM
445-019
MONITOR POSITION
WISI
9SEI
EISIO
18SWI
1
2
4
8
16
32
64
128
TRIG DELAY
e+
MONITOR POSITION
WISI
9SEI
EISIO
18SWI
TRIG DELAY
e−
102 MHZ INPUT
TRIGGER INPUT
DELAYED OUTPUTS
e+
DELAYED OUTPUTS
e−

FIG. 14

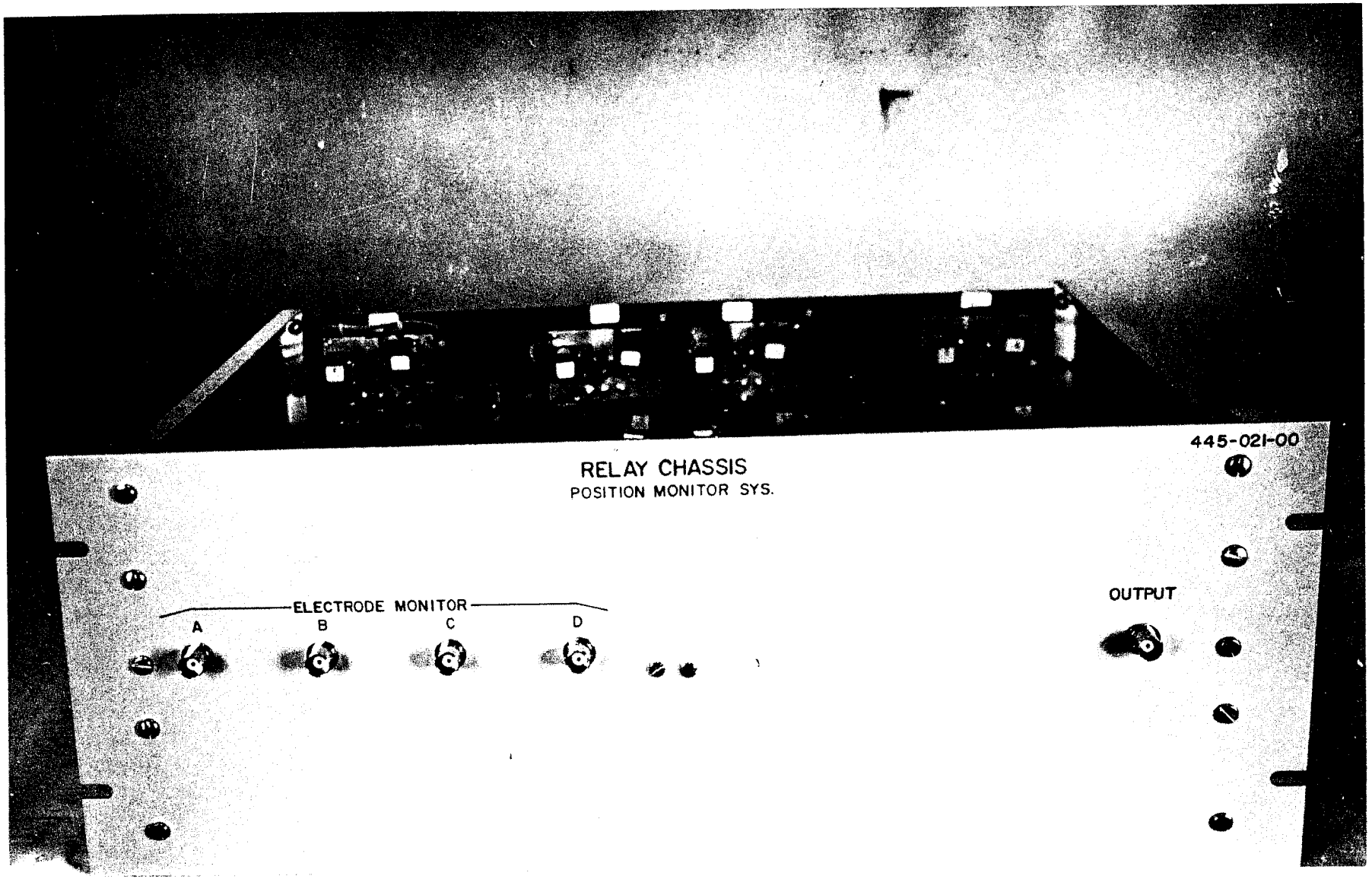
445-021-00
RELAY CHASSIS
POSITION MONITOR SYS.
ELECTRODE MONITOR
A
B
C
D
OUTPUT

FIG. 15